Harnessing vacuum forces for quantum sensing of graphene motion

Christine A. Muschik[1], Simon Moulieras[1], Maciej Lewenstein[1,2], Frank Koppens[1], and Darrick Chang[1]
[1] *ICFO-Institut de Ciències Fotòniques, Mediterranean Technology Park, 08860 Castelldefels (Barcelona), Spain*
[2] *ICREA - Institució Catalana de Recerca I Estudis Avançats, Lluis Companys 23, E-08010 Barcelona, Spain*

The existence of vacuum forces [1, 2] is one of the most striking consequences of quantum mechanics. We show how the strong potentials induced by vacuum fluctuations can be exploited in a practical scheme for quantum sensing. Position measurements at the quantum level are of central importance for many applications but very challenging. Typically, methods based on optical forces are used [3], but these are generally weak and difficult to apply to many materials. An important example is graphene, which is an excellent mechanical resonator due to its low mass and whose unique properties render it an outstanding platform for nanotechnologies [4–6]. We describe a protocol wherein quantum vacuum potentials yield a strong dispersive interaction between the displacement of a graphene nanomechanical resonator and a nearby quantum optical emitter. This interaction yields a large position-dependent shift in the transition frequency of the emitter, which can be read out via an optical field. Under realistic conditions, we show that this mechanism enables strong quantum squeezing of the graphene position on time scales short compared to the mechanical period.

Quantum vacuum forces cause attraction between two uncharged objects due to the modification of the zero-point energy in the space between them [1, 2]. They become extremely strong at very short distances, which is considered to be a major problem: Casimir forces prevent the trapping of particles close to surfaces and lead to "stiction", which complicates considerably the fabrication and handling of nano devices. Therefore, they are commonly believed to be "one of the most important reliability problems in micro-electromechanical systems" [7].

However, one can also envision that the strength of vacuum forces enables them to be exploited for applications. A spectacular but extremely challenging example is the attempt to engineer repulsive Casimir forces for frictionless devices and quantum levitation [2, 8]. Here, we present an application possible with current experimental capabilities and without the need to create repulsion. Specifically, our scheme harnesses Casimir potentials for fast and precise position measurements of a mechanical object [3, 9–11], which is needed for a plethora of applications, including the measurement of small forces. This is a radically new concept, which is not only very interesting from a fundamental point of view but also practically advantageous, since the strength of the employed mechanism allows for an enhanced sensitivity and drastically increased speed of the measurement. The use of quantum vacuum potentials therefore enables one to access new regimes that are not possible with traditional methods.

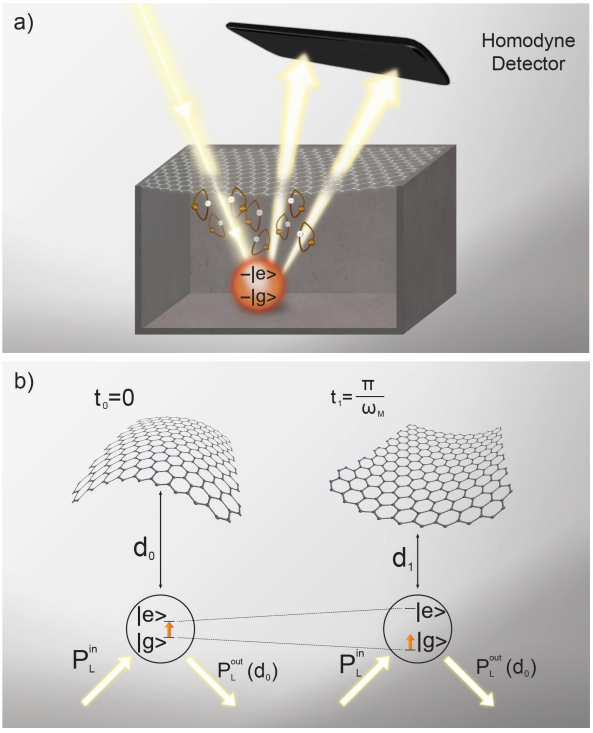

FIG. 1: Motion sensing via quantum vacuum potentials: a) A stationary quantum emitter with internal states $|e\rangle$ and $|g\rangle$ is located in the vicinity of a suspended graphene sheet and illuminated by a laser field. Vacuum fluctuations (as illustrated by the loops) affect the transition frequency of the emitter, while the scattered light field is measured by means of homodyne detection. b) The graphene membrane and the quantum system interact via the vacuum potential: the energy levels of the emitter are shifted depending on its distance d to the membrane. The distance-dependent level shift translates into a phase shift of the light and can be read-out by measuring the p-quadrature of the scattered field.

As an example, we show that our technique allows for nearly "instantaneous" position measurements, which is very difficult to achieve with other experimental schemes. Specifically, our protocol facilitates the monitoring of the motion of the membrane at the quantum level in real-time, *i.e.*, on a time scale which is short compared to the mechanical oscillation period. This possibility

paves the way for studying the mechanical response at fast time scales and for quantum squeezing of the position uncertainty of the mechanical system.

A specifically interesting material in this context is graphene due to its small mass and high Q-factor [6]. However, to date no technique for position measurements on the quantum level is available for graphene. Due to its weak and broadband absorption of 2.3% [12], methods based on optical forces [3] are not suitable. Typically, capacitive techniques are used [6, 13, 14], which measure the position averaged over many cycles of the mechanical motion.

We exploit the strong Casimir interaction between a dipolar emitter and graphene and consider a suspended moving membrane which is coupled via the Casimir potential to a two level system with fixed position as shown in Fig. 1a (also compare with Ref. [15]). The paradigmatic example of the Casimir effect is the (typically attractive) force between two surfaces, due to the modification of the electromagnetic vacuum energy density in the intervening space. A similar mechanism governs the interaction between a surface and a single quantum emitter: quantum vacuum fluctuations lead to a modification of the energy of each electronic state, which depends on the presence of nearby surfaces. A moving atom would therefore experience a force associated with the derivative of these shifts [16, 17]. A stationary emitter on the other hand experiences a measurable change in its resonance frequency that depends on the distance to the surface. Mechanical displacements can subsequently be read out by detecting the changing phase shift of a coherent field scattered from the emitter, as illustrated in Fig. 1b.

The Casimir potential for an emitter in its electronic ground state at position $\mathbf{r}$ can be calculated [16, 17] by considering the interaction of the emitter with the vacuum modes of the electromagnetic field via the dipole Hamiltonian $H_{\rm dip} = -\mathbf{d}\cdot\mathbf{E}(\mathbf{r}) = -\sum_k g_k(\mathbf{r})(|e\rangle\langle g| + |g\rangle\langle e|)(a_k + a_k^\dagger)$, where $\mathbf{d}$ is the dipole moment of the emitter and $\mathbf{E}(\mathbf{r})$ is the electromagnetic field at position $\mathbf{r}$ with normal modes k. We consider here a two-level system with ground and excited state $|g\rangle$ and $|e\rangle$. g_k denotes the vacuum Rabi coupling strength between the emitter and normal mode k with creation operator $a_k^\dagger$ and frequency ω_k. This Hamiltonian contains terms which enable an atom in its ground state to couple virtually to the excited state and create a photon $|g,0\rangle \rightarrow |e,1_k\rangle$, which can be scattered from the surface before it is reabsorbed. The corresponding frequency shift of the ground state due to these quantum fluctuations is given by $\delta\omega_g(\mathbf{r}) = -\sum_k g_k(\mathbf{r})^2/(\omega_0+\omega_k)$, where ω_0 is the resonance frequency in free space. The shift can be re-expressed in terms of the classical (dyadic) electromagnetic Green's function $G(\mathbf{r},\mathbf{r},iu)$ [18] evaluated at

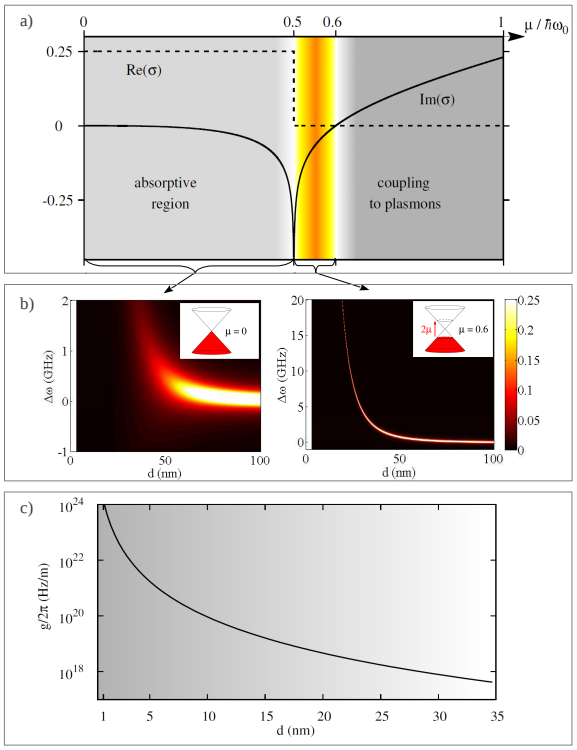

FIG. 2: Optical properties of graphene and resulting frequency shifts on a nearby quantum emitter: a) Conductivity σ of doped graphene versus Fermi energy μ in units of $\hbar\omega_0$, where ω_0 is the resonance frequency of the emitter. The real part of the conductivity (dashed line) describes absorption. For $\frac{\mu}{\hbar\omega_0} < 0.5$, light radiated by the emitter is absorbed since photons with frequency $\hbar\omega \geq 2\mu$ can induce inter band transitions. For $\mu/\hbar\omega_0 > 0.6$, $\mathrm{Im}(\sigma) > 0$, which implies that the emitter can couple to surface plasmons. This type of process is undesired since it increases the non-radiative decay rate of the emitter; b) The effects of the Casimir-induced level shift $\Delta\omega$ and modified spontaneous emission rate Γ versus distance d can be seen in the total photon scattering rate of an emitter. Here we take a free-space emission rate and wavelength $\Gamma_0 = 2\pi \times 160$ MHz and $\lambda_0 = 2\cdot 10^{-6}$m. The left and right panels correspond to $\mu = 0$ and $\mu = 0.6\hbar\omega_0$, respectively. For a fixed distance, the scattering rate in the limit of weak excitation power exhibits a Lorentzian frequency response $f(\omega,d) \propto \frac{\Gamma/2}{(\omega-\Delta\omega(d))^2+(\Gamma/2)^2}$, which here is normalized by the maximal value $f_{\max}(\omega,d)$. The total linewidth Γ and center frequency $\Delta\omega(d)$ (relative to $d\rightarrow\infty$) change versus distance d due to the modified spontaneous emission rate and Casimir shifts, respectively. c) Optomechanical coupling coefficient $g = \frac{\partial\omega}{\partial d}$ in $\frac{\mathrm{Hz}}{\mathrm{m}}$ versus the distance d in nm for the Fermi energy $\mu = 0.6\hbar\omega_0$ that yields the optimal effective coupling κ for the parameters considered in Fig. 3.

imaginary frequencies $\omega = iu$,

$$\delta\omega_g(\mathbf{r}) = \frac{3c\Gamma_0}{\omega_0^2}\int_0^\infty du \frac{u^2}{\omega_0^2+u^2}\mathrm{Tr}\{G(\mathbf{r},\mathbf{r},iu)\},$$

where c is the speed of light and Γ_0 is the emission rate of the emitter in free space. Similar calculations allow

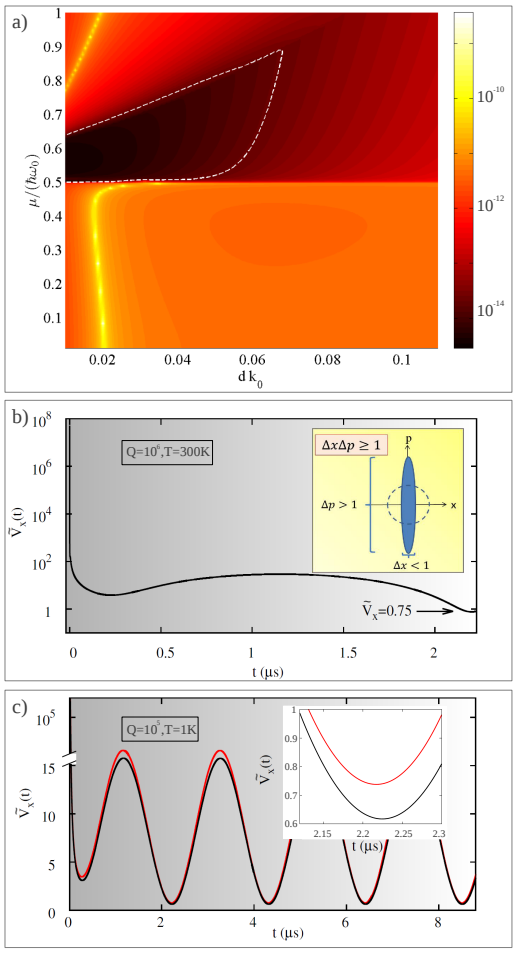

FIG. 3: Casimir-sensitivity and creation of position squeezing starting from a thermal state: a) Inverse coupling strength κ^{-1} in $\frac{\sqrt{\text{Hz}}}{\text{m}}$ versus the distance d and the Fermi energy μ in units of $\hbar\omega_0$, where ω_0 is the resonance frequency of the emitter in free space. In the region within the dashed line, the sensitivity is better than the standard quantum limit $S_{xx} = \sqrt{\frac{\hbar Q}{m\omega_{\text{M}}}}$ for a quality factor $Q = 1$; b,c) $V_x(t)$, the conditional variance of the position in the rotating frame and in units of the zero point fluctuations of the oscillator x^2_{ZPM} versus time in μs. b) shows the rapid generation of a squeezed state (see inset) at room temperature $T = 300K$, during a short time window for pure momentum damping at $Q = 10^6$. Panel c) depicts $V_x(t)$ during several oscillation periods for $T = 1\text{K}$ and $Q = 10^5$. The red and black lines correspond to symmetric damping $\gamma_x = \gamma_p = \gamma/2$ and momentum damping $\gamma_x = 0, \gamma_p = \gamma$ respectively. The results in this figure have been calculated for a graphene sheet with resonance frequency $\omega_M = 2\pi \times 240$ kHz, mass $m = 5.6 \cdot 10^{-18}$kg, Fermi level $\mu = 0.6\hbar\omega_0$ and an emitter at a distance $d = 10$nm with free space emission rate $\Gamma_0 = 2\pi \times 160$ MHz and wavelength $\lambda_0 = 2 \cdot 10^{-6}$m. $\nu_{\text{det}} = 0.5$ and $\epsilon = \frac{\Omega^2}{\Delta^2+\Gamma^2} = 0.2$, where Ω is the Rabi frequency of the applied laser field and Δ is the detuning.

one to determine the excited-state shift $\delta\omega_e$ and modified emission rate $\Gamma(\mathbf{r})$ near the surface [19].

At distances d that are much closer than the free-space resonant wavelength λ_0, the shift in the transition frequency of the emitter typically scales like $\Delta\omega = \delta\omega_e - \delta\omega_g \propto \Gamma_0/(dk_0)^3$ for a bulk conductor and like $\Delta\omega \propto \Gamma_0\alpha/(dk_0)^4$ for graphene, where α is the fine structure constant and $k_0 = 2\pi/\lambda_0$. This divergent nature implies that the properties of the emitter change very strongly at short distances, which is the basis of our extremely sensitive detection scheme.

Fig. 2a depicts the AC-conductivity of graphene [12], which characterizes the optical properties of the material and the corresponding Casimir potential induced level shifts. The exact values of the level shifts depend on the Fermi energy μ, which can be tuned by varying the level of doping. This can be done either electrically by applying a gate voltage or chemically by introducing impurities. The frequency shift $\Delta\omega$ is shown in Fig. 2b in the absence of doping $\mu = 0$, and for the Fermi energy $\mu = 0.6\hbar\omega_0$ that is found to yield the optimal read-out sensitivity for the considered parameters, as will be explained below.

We describe the suspended membrane as a quantum mechanical harmonic oscillator with position x_M, momentum p_M, and commutation relation $[x_M, p_M] = i\hbar$. For small displacements x_M, the Hamiltonian which describes the position-dependent frequency of the emitter can be expanded up to first order in x_M, $H_{\text{emitter}} = \hbar\omega_{eg}(x_M)\sigma_z = \hbar\left(\omega_{eg}(0) + \frac{\partial\omega_{eg}(x_M)}{\partial x_M}x_M\right)\sigma_z + O(x_M^2)$, such that

$$H_{\text{emitter}} = H^0_{\text{emitter}} + \hbar g x_M \sigma_z,$$

where $\sigma_z = |e\rangle\langle e| - |g\rangle\langle g|$. $\omega_{eg}(0)$ is the level splitting at the distance that is associated with the equilibrium position $x_{\text{M}} = 0$. The optomechanical coupling coefficient g, given by $g = \frac{\partial\omega_{eg}(x_M)}{\partial x_M}$, describes the rate of change of the emitter freuqency per unit displacement and is shown in Fig. 2c. As a concrete example, we consider here an emitter with $\Gamma_0 = 2\pi \times 160$ MHz and $\lambda_0 = 2 \cdot 10^{-6}$m placed at a distance $d = 10$nm from a graphene sheet with with resonance frequency $\omega_M = 2\pi \times 240$ kHz, mass $m = 5.6 \cdot 10^{-18}$kg and Fermi energy $\mu = 0.6\hbar\omega_0$. In this case, $g = 2\pi \times 0.81 \cdot 10^{11}\frac{\text{GHz}}{\text{m}}$ and the resonance frequency of the emitter shifts by $2\pi \times 0.27$ GHz, if the graphene sheet is displaced by one unit of zero point motion $x_{\text{ZPM}} = \sqrt{\frac{\hbar}{m\omega_M}} = 3.4 \cdot 10^{-12}$m. This coupling coefficient compares very favorably to the best demonstrated couplings in cavity opto-mechanics experiments [20] and provides the basis for our very sensitive detection scheme.

We discuss this sensitivity in the following by considering a read-out of the level shift by means of a coherent light field in the weak driving limit (when population of the atomic excited state is negligible). This limit is characterized by $\epsilon = \frac{\Omega^2}{\frac{\Gamma^2}{4}+\Delta^2} \ll 1$, where Ω is the Rabi

frequency of the applied laser field and Δ is the laser detuning at $x_M = 0$. Physically, working in the limit of $\epsilon \ll 1$ enables the mechanical interaction with the two-level system to be linearized and ensures that the optical scattering from the emitter is predominantly coherent.

The applied light field interacts with the emitter via the dipole Hamiltonian $H = -\mathbf{d}\cdot\mathbf{E}$ and carries information about the atomic coherence after the interaction. In particular, the input and output (scattered) fields are related to the atomic coherence via the relation $a_{\rm L}^{\rm out} = -a_{\rm L}^{\rm in} + \sqrt{\nu\Gamma}\,|g\rangle\langle e|$, where ν characterizes the detection efficiency. This way, phase fluctuations in the atomic coherence are mapped to phase fluctuations of the scattered light field. In the weak driving limit, the emitter can be adiabatically eliminated. This yields an effective emitter-mediated interaction between the membrane and the light field. The latter is described in terms of its quadratures $x_{\rm L} = (a_L + a_L^\dagger)/\sqrt{2}$ and $p_{\rm L} = -i(a_L - a_L^\dagger)/\sqrt{2}$ such that the membrane evolves under the Hamiltonian

$$\begin{aligned} &H_{\rm membrane} = H_{\rm M} + H_{\rm ML}, \qquad (1)\\ &H_{\rm M} = \frac{\hbar}{2m}p_{\rm M}^2 + \frac{\hbar}{2}m\omega_{\rm M}^2 x_{\rm M}^2, \quad H_{\rm ML} = \hbar\kappa\, x_M p'_{\rm L}, \end{aligned}$$

where $p'_{\rm L} = -\frac{\bar\beta}{\sqrt{\epsilon}}x_{\rm L} + \frac{\bar\alpha}{\sqrt{\epsilon}}p_{\rm L}$ with $\bar\alpha = \Omega\frac{\Gamma}{2}/(\Delta^2 + \frac{\Gamma^2}{4})$ and $\bar\beta = \Omega\Delta/(\Delta^2 + \frac{\Gamma^2}{4})^2$. The effective coupling constant κ is a central quantity of the sensing scheme. It is given by $\kappa = \bar g\sqrt{\epsilon\nu/\Gamma}$, where $\bar g = \frac{g}{\sqrt{2}}\left(1 - \frac{3}{8}\epsilon\right)$ is a renormalized coupling coefficient.

In the case of ideal detection efficiency, the rate at which information about $x_{\rm M}$ (in vacuum units $x_{\rm ZPM}$) can be collected is given by $\kappa^2_{\rm ideal} = \frac{\epsilon\bar g^2 x^2_{\rm ZPM}}{\Gamma}$. Since we are interested in measuring the mechanical motion on time scales which are short compared to $\omega_{\rm M}^{-1}$, the dimensionless quantity $\frac{\kappa^2_{\rm ideal}x^2_{\rm ZPM}}{\omega_{\rm M}} = \frac{\epsilon(\bar g\cdot x_{\rm ZPM})^2}{\Gamma\omega_M}$ represents an important reference value for assessing the potential of the scheme to measure motion at the quantum level for any combination of emitter and membrane parameters.

The basic working principle of the scheme can be understood by considering the dynamics in the absence of undesired processes (which will be addressed below) during a short time window $\Delta t \ll \omega_{\rm M}^{-1}$. In this case, $H_{\rm ML}$ leads to a simple mapping of the mechanical position $x_{\rm M}$ onto the light field

$$\begin{aligned} x_L'^{\rm out} &= x_L'^{\rm in}, & x_M^{\rm out} &= x_M^{\rm in},\\ p_L'^{\rm out} &= p_L'^{\rm in} + \kappa x_M^{in}, & p_M^{\rm out} &= p_M^{in} + \kappa x_L'^{\rm in}, \end{aligned}$$

where the superscripts "in" and "out" denote operators before and after the interaction. If p'_L is measured using homodyne detection, $x_{\rm M}$ can be inferred in an optimal fashion and a highly position squeezed state with variance $V_x(t) = \frac{1}{(V_x^{\rm in})^{-1} + \kappa^2 t}$ is generated.

The dynamics considered here is more complicated due to the presence of the free Hamiltonian of the membrane $H_{\rm M} = \frac{\hbar}{2m}p_{\rm M}^2 + \frac{\hbar}{2}m\omega_{\rm M}^2 x_{\rm M}^2$, mechanical damping and due to loss mechanisms that are associated with the light-atom interaction and the imperfect detection of the light field. We consider two different types of damping: a symmetric damping model, where position and momentum are damped with equal rates $\gamma_x = \gamma_p = \gamma/2$, and for pure momentum damping $\gamma_x = 0$, $\gamma_p = \gamma$. In the latter case, almost noise-free position measurements can be made in the short time limit, *i.e.*, if the chosen measurement time Δt is short on the time scale of the mechanical rotation in phase space, since position damping requires a time span on the order of ω_M^{-1} to affect the mechanical position.

In the following, we evaluate the performance of the sensing scheme for the specific example of a suspended graphene sheet. For the parameter set introduced above and $\epsilon = 0.2$ we obtain $\kappa^{-1} = 1.4\cdot 10^{-15}\frac{\rm m}{\sqrt{\rm Hz}}$. The sensitivity of the Casimir sensing technique κ^{-1} is below the standard quantum limit $S_{xx} = \sqrt{\frac{\hbar Q}{m\omega_{\rm M}^2}} = \sqrt{Q}\cdot 2.8\cdot 10^{-15}\frac{\rm m}{\sqrt{\rm Hz}}$, where Q is the quality factor associated with the graphene membrane [21]. Fig. 3a displays κ^{-1} versus the distance d and the Fermi energy μ. It shows that the optimal read-out rate can be achieved for Fermi energies between $\mu = 0.5\hbar\omega_0$ and $\mu = 0.6\hbar\omega_0$. This dependence on Fermi energies is due to the maximum possible detection efficiency ν. In particular, $\nu = \eta_{\rm det}\frac{\Gamma_{\rm rad}}{\Gamma}$ contains one term $\eta_{\rm det}$ describing the efficiency at which photons scattered in free space can be collected, and is technical in nature. The other term, $\frac{\Gamma_{\rm rad}}{\Gamma}$, describes the probability for a photon to be scattered to free space, as compared to being absorbed by the material. The dependence of the latter quantity on μ can be understood by considering the optical properties of graphene shown in Fig. 2a. For $\mu < 0.5\hbar\omega_0$, the graphene sheet is highly absorptive, as light can induce inter-band electronic transitions. For high Fermi levels ($\mu > 0.6\hbar\omega_0$) on the other hand, a different "absorption" mechanism occurs, as graphene acts like a thin conducting film and supports highly localized guided surface plasmons. The emitter can efficiently couple to these guided modes, which are dark to free-space detection channels. In either case, the non-radiative emission rate $\Gamma_{\text{non-rad}} = \Gamma - \Gamma_{\rm rad}$ of an emitter close to a graphene sheet increases drastically for short distances [22–24], resulting in little energy radiated in the form of photons.

The ability to perform a strong read-out of the position $x_{\rm M}$ on time scales that are short compared to $\omega_{\rm M}^{-1}$ allows one create a squeezed state where the variance of the position of the graphene sheet is reduced below its value in the vacuum state $V_x < x^2_{\rm ZPM}$ at the expense of increasing the variance of the conjugate variable in compliance with the Heisenberg uncertainty principle $V_x\cdot V_p \geq \hbar/4$ (see Fig. 3b). The rotation in phase space would prevent the squeezing of x_M or p_M, if measurements over several oscillation periods were

required, but since the high coupling strength κ allows for a fast and precise read-out, the Casimir scheme yields significant squeezing even at room temperature (see inset in Fig. 3b). Moreover, the high sensitivity of the scheme renders the distinction between different types of damping possible. Symmetric and moment damping would become indistinguishable if averaged over several oscillation periods, but lead to different results if a high temporal resolution is available, as shown in Fig. 3c.

In summary, we have shown that strong quantum vacuum interactions can be used as a valuable resource for the measurement of nanomechanical systems at the quantum level. We have specifically analyzed our protocol for the case of a graphene nanomechanical resonator, which is viewed as a promising platform for devices but currently lacks the means for fast readout. However, in principle, the presented method is quite general and can be applied to a wide class of materials. If the position of the mechanical object to the quantum emitter is known, our scheme allows for a precise study and measurement of Casimir forces [25–29] at a level of precision that has not been possible so far. The ability to measure Casimir forces accurately is an important step towards the vision of controlling and manipulating quantum vacuum potentials.

Acknowledgements

We gratefully acknowledge discussions with Adrian Bachtold and Joel Moser and Ignacio Cirac. This work was supported by the ERC grants QUAGATUA and CARBONLIGHT, the Alexander von Humboldt Foundation, TOQATA (FIS2008-00784), Fundació Privada Cellex Barcelona and the EU integrated projects AQUTE and SIQS.

[1] Casimir, H. G. B. On the attraction between two perfectly conducting plates. *Proc. Con. Ned. Akad. van Wet* **51**, 793–796 (1948).

[2] Lamoreaux, S. K. The Casimir force: background, experiments and applications. *Rep. Prog. Phys.*, **68**, 201–236 (2005).

[3] Aspelmeyer, A., Groblacher, S., Hammerer, K., & Kiesel, N. Quantum optomechanics – throwing a glance. *J. Opt. Soc. Am. B* **27**, A189–A197 (2010).

[4] Bunch, J. S., van der Zande, A. M., Verbridge, S. S., Frank, I. W., Tanenbaum, D. M., Parpia, J. M., Craighead, H. G. & McEuen, P. L. Electromechanical resonators from graphene sheets. *Science* **315**, 490–493 (2007).

[5] Chen, C., Rosenblatt, S., Bolotin, K. I., Kalb, W., Kim, P., Kymissis, I., Stormer, H. L., Heinz, T. F., & Hone, J. Performance of monolayer graphene nanomechanical resonators with electrical readout. *Nature Nanotech.* **4**, 861–867 (2009).

[6] Eichler, A., Moser, J., Chaste, J., Zdrojek, M., Wilson-Rae, I., & Bachtold, A. Nonlinear damping in mechanical resonators made from carbon nanotubes and graphene. *Nature Nanotech.* **6**, 339–342 (2011).

[7] van Spengen, W. M., Puers, R. & De Wolf, I. A physical model to predict stiction in MEMS. *J. Micromech. Microeng.* **12**, 702 (2002).

[8] Munday, J. N., Capasso, F. & Parsegian, V. A. Measured long-range repulsive CasimirLifshitz forces. *Nature* **457**, 170–173 (2009).

[9] Arcizet, O., Jacques, V., Siria, A., Poncharal, P., Vincent, P. & Seidelin, S. A single nitrogen-vacancy defect coupled to a nanomechanical oscillator. *Nature Phys.* **7**, 879–883 (2011).

[10] Kolkowitz, S., Bleszynski Jayich, A. C., Unterreithmeier, Q. P., Bennett, S. D., Rabl, P., Harris, J. G. E. & Lukin, M. D. Coherent sensing of a mechanical resonator with a single-spin qubit. *Science* **30**, 1603–1606 (2012).

[11] Puller, V., Lounis, B. & Pistolesi, F. Single molecule detection of nanomechanical motion. Preprint at http://arxiv.org/abs/1211.4463.

[12] Stauber, T., Peres, N. & Geim, A. Optical conductivity of graphene in the visible region of the spectrum. it Phys. Rev. B **78**, 085432 (2008).

[13] Gouttenoire, V., Barois, T., Perisanu, S., Leclercq, J.-L., Purcell, S. T., Vincent, P., & Ayari, A. Digital and FM demodulation of a doubly clamped single-walled carbon-nanotube oscillator: towards a nanotube cell phone. *Small* **6**, 1060–1065 (2010).

[14] Xu, Y., Chen, C., Deshpande, V.V., DiRenno, F. A., Gondarenko, A., Heinz, D. B., Liu, S., Kim, P., & Hone, J. Radio frequency electrical transduction of graphene mechanical resonators. *App. Phys. Lett.* **97**, 243111 (2010).

[15] Ribeiro, S. & Scheel, S. Controlled ripple texturing of suspended graphene membrane due to coupling with ultracold atoms. preprint available at http://arxiv.org/abs/1303.1711.

[16] Buhmann, S. Y., Knöll, L., Welsch, D.-G. & Dung, H. T. Casimir-Polder forces: A nonperturbative approach *Phys. Rev. A*, **70**, 052117 (2004).

[17] Buhmann, S. Y. & Welsch, D.-G. Dispersion forces in macroscopic quantum electrodynamics. *Prog. Quantum Electron.* **31**, 51-130 (2007).

[18] The Green's function $G(\mathbf{r}, \mathbf{r}', \omega)$ is defined through the relation $\left[(\nabla \times \nabla \times) - \frac{\omega^2}{c^2}\epsilon(\mathbf{r}, \omega)\right] G(\mathbf{r}, \mathbf{r}', \omega) = \delta(\mathbf{r}–\mathbf{r}') \otimes \mathbb{1}$.

[19] Schiefele,J. & Henkel, C. Bosonic enhancement of spontaneous emission near an interface. *Phys. Rev. A* **375**, 680–684 (2011).

[20] Safavi-Naeini, A.H., Alegre, T.P.M., Winger, M. & Painter, O. Optomechanics in an ultrahigh-Q two-dimensional photonic crystal cavity. *Appl. Phys. Lett.* **97**, 181106 (2010).

[21] The comparison of the inverse coupling stergth κ^{-1} with the standard quantum limit $S_{xx} = \frac{\hbar Q}{m\omega_{\mathrm{M}}^2}$ relates the measurement sensitivity with the time and length scales of the considered oscillator in its ground state. $\kappa^{-1} < S_{xx}$ indcates that the motion of the membrane can be mea-

sured at the quantum level. No statement regarding the evasion of backaction on the measured system is implied here.

[22] Koppens, F. H. L., Chang, D. E. & Garcia de Abajo, F. J. Graphene plasmonics: a platform for strong light-matter interactions. *Nano Lett.* **11**, 3370–3377 (2011).

[23] Nikitin, A. Y., Guinea, F., García-Vidal, F. & Martín-Moreno, L. Fields radiated by a nanoemitter in a graphene sheet. *Phys. Rev. B* **84**, 195446 (2011).

[24] Gaudreau, L., Tielrooij, K. J., Prawiroatmodjo, G. E. D. K., Osmond, J., García de Abajo, F. J. & Koppens, F. H. L. Universal distance-scaling of nonradiative energy transfer to graphene. *Nano Lett.* online publication, DOI:10.1021/nl400176b (2013).

[25] Sukenik, C. I., Boshier, M. G., Cho, D., Sandoghdar, V. & Hinds, E. A. Measurement of the Casimir-Polder force. *Phys. Rev. Lett.* **70**, 560–563 (1993).

[26] Landragin, A., Courtois, J.-Y., Labeyrie, G., Vansteenkiste, N., Westbrook, C. I. & Aspect, A. Measurement of the van der Waals Force in an atomic mirror. *Phys. Rev. Lett.* **77**, 1464–1467 (1996).

[27] Munday, J. N. & Capasso, F. Precision measurement of the Casimir-Lifshitz force in a fluid. *Phys. Rev. A* **75**, 060102(R), (2007).

[28] Bender, H., Courteille, Ph. W., Marzok, C., Zimmermann, C., &S. Slama S. Direct measurement of intermediate-range Casimir-Polder potentials. *Phys. Rev. Lett.* **104**, 083201 (2010).

[29] Alton, D. J., Stern, N. P., Aoki, T., Lee H., Ostby, E., Vahala, K. J. & Kimble, H. J. Strong interactions of single atoms and photons near a dielectric boundary. *Nature Phys.* **7**, 159–165 (2011).